Passively Mode-Locked Fiber Lasers Based on Nonlinearity at 2-μm Band

Tianshu Wang, *Member, IEEE*, Wanzhuo Ma, Qingsong Jia, Qingchao Su, Peng Liu, and Peng Zhang

(Invited Paper)

***Abstract*—2-μm fiber lasers are of wide potential applications in the fields of radar, sensing, and free-space communications. We introduced a simple approach to generate passively mode-locked pulse in thulium-doped fiber lasers based on nonlinear polarization rotation (NPR) in our previous work. The high repetition rate of 1.78 GHz is obtained by both NPR and semiconductor saturable absorption mirror. By using a polarization-maintaining fiber in the experiment, a birefringence Lyot filter as a fiber comb filter can be constructed, and then the tuning range of 94 nm can be obtained for the mode-locked laser. In this paper, we also demonstrated our recent research work, a square-wave mode-locked fiber laser at 2-μm band based on nonlinear amplifying loop mirror. The square-wave noiselike pulse (NLP) at longer wavelength of 2-μm band can be observed. With the increase of the pump power, pulse width can be increased from 0.75 to 1.3 ns. The polarization vector characteristics of the square-wave NLP were analyzed experimentally. In addition, with the increase of the pump power, a kind of square-wave mode-locked pulse with low-intensity multipulse bunches can be observed, and these multipulse bunches can be operated at the multipulse mode-locked state. The side-mode suppression ratio decreased from 50 to 30 dB.**

***Index Terms*—Fiber laser, 2 μm band, mode-locking, nonlinear polarization rotation, nonlinear amplifying loop mirror.**

I. Introduction

RECENTLY, fiber lasers operating around 2 μm region have been becoming research focus because of eye safe and high transmissivity in organic gas. In addition, mode-locked fiber lasers are becoming more and more popular. Although most reports of mode-locked fiber lasers are about 1 μm and 1.55 μm band, more important mode-locked fiber lasers at 2 μm band have attracted great research interests because of their potential applications in laser medicine, LIDAR, free space laser communications, optical sensing, optoelectronic countermeasure and mid-IR supercontinuum generation [1]–[6]. Passively mode-locking is an effective method to obtain mode-locked fiber lasers at 2 μm band, and there are several typical techniques to achieve passive mode-locking, including saturable absorber [7], [8], nonlinear polarization rotation (NPR), nonlinear optical loop mirror (NOLM) [9] and nonlinear amplifying loop mirror (NALM) [10]–[15]. In recent years, 2 μm band mode-locked fiber lasers develop rapidly, tunable multi-wavelength [9], harmonic mode-locking [12] and single pulse train [15] can be obtained while using mode-locked fiber lasers based on NPR and NALM. Since 2 μm band fiber laser with simple structure and low maintenance cost can be achieved, it has obvious advantages in industrial application.

Up to now, the most conventional approaches to achieve radiation around 2 μm band are using pumped thulium-doped, holmium-doped or thulium/holmium co-doped fibers, and the related studies have been reported in the past few years [16]–[18]. The use of the Tm^{3+} ion for 2 μm band fiber laser applications has been wide spread mainly as a result of the convenient absorption band near 1.55 μm which allows for fiber laser pumping. Similarly, Tm^{3+}/Ho^{3+} ion-pair can be pumped by 1.55 μm lasers, and optical gain band can extend to longer wavelengths.

In this paper, we introduce our previous works about 2 μm band passively mode-locked thulium-doped fiber lasers based on NPR in Section II. The high repetition rate with 1.78 GHz can be observed, and furtherly, mode-locked fiber lasers can be tuned with a range of 94 nm through adding a polarization maintain fiber (PMF). Then, in Section III, we demonstrate a kind of mode-locked thulium/holmium co-doped fiber laser by using a NALM in our recent research work. A square-wave noise-like pulse (NLP) can be observed at 2 μm band, and square-wave mode-locked pulse with low intensity multi-pulse bunches can be generated with high pump power.

II. Mode-Locked Tm-Doped Fiber Lasers Based on NPR

Nonlinear polarization rotation effect has been widely used as saturable absorber due to its characteristics of intensity-dependent transmission. Picosecond or femtosecond pulses can

Manuscript received July 31, 2017; revised October 3, 2017; accepted December 8, 2017. Date of publication December 18, 2017; date of current version February 7, 2018. This work was supported in part by the National Science Foundation of China under Grant 60907020, in part by the Nature Science Fund of Jilin Province under Grant 20150101044JC, and in part by the Science and Technology Project of Jilin Province under Grant 20170414041GH. *(Corresponding author: Tianshu Wang.)*

T. Wang and P. Zhang are with the National and Local Joint Engineering Research Center of Space Optoelectronics Technology, Changchun University of Science and Technology, Changchun 130022, China (e-mail: wangts@cust.edu.cn; zhangpeng@cust.edu.cn).

W. Ma and Q. Jia are with the College of Opto-Electronic Engineering, Changchun University of Science and Technology, Changchun 130022, China (e-mail: wanzhuoma@126.com; 740909697@qq.com).

Q. Su and P. Liu are with the College of Science, Changchun University of Science and Technology, Changchun 130022, China (e-mail: 2510231643@qq.com; 751853793@qq.com).

Color versions of one or more of the figures in this paper are available online at http://ieeexplore.ieee.org.

Digital Object Identifier 10.1109/JSTQE.2017.2783047

1077-260X © 2018 IEEE. Translations and content mining are permitted for academic research only. Personal use is also permitted, but republication/redistribution requires IEEE permission. See http://www.ieee.org/publications_standards/publications/rights/index.html for more information.

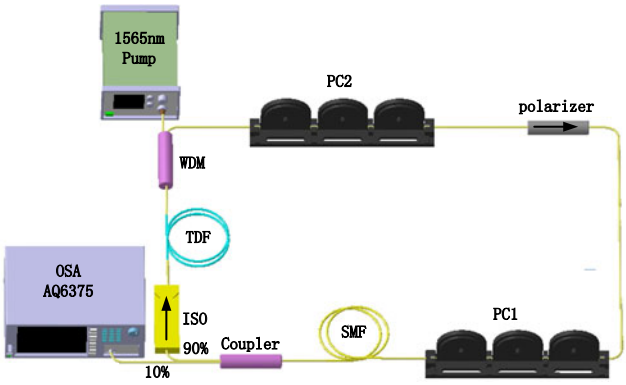

Fig. 1. Configuration of thulium-doped mode-locked fiber laser based on NPR. PC, polarization controller; SMF, single-mode fiber; OC, optical circulator; TDF, thulium-doped fiber; WDM, wavelength division multiplexer; PD, photodetector; OSA, optical spectrum analyzer; ESA, electrical spectrum analyzer.

be obtained by using spatial NPR structure since it was firstly applied in passive mode-locked fiber lasers in 1992 [19]. Therefore, the nonlinearity is important for mode-locked fiber lasers based on NPR. As we know, increasing the length of the fiber in resonant cavity is an effective way to improve the nonlinearity. But using additional fiber length to enhance the nonlinear effect always leads to pulse broadening. Thus dispersion management has been widely investigated to achieve ultrafast optical pulses in all-fiber NPR-based passive mode-locked fiber lasers. Even so achieving 2 μm all-fiber ultrafast mode-locked laser is still difficult due to the lack of dispersion management devices at this region comparing with 1 μm and 1.55 μm band. NPR structure can affect the cavity loss, thus it has advantages to achieve a widely tunable continuous-wave or mode-locked fiber laser [20], [21]. In addition, NPR structure is sensitive to dispersion and nonlinearity in the cavity. Therefore, by appropriately adjusting parameters in the cavity, we can produce versatile pulse patterns such as dissipative solitons [22], dissipative soliton resonance [23], bound state pulses [24], vector solitons [25] and harmonic mode-locked laser [26]. However, these related reports mainly focus on 1.55 μm and 1 μm region.

In this section, we introduce our previous research works about mode-locked fiber laser in 2 μm region by using NPR. In the experiments, a mode-locked fiber laser pulse with a high repetition rate of 1.78 GHz can be observed, and a wide tunable mode-locked fiber laser at 2 μm band with tuning range of 94 nm can be obtained.

A. Experimental Setup and Principle

In passively mode-locked fiber lasers based on NPR, low intensity light is absorbed and high intensity light gets through when the light pass through NPR structure, and it is oscillated continually in the cavity [27]. Therefore, the mode-locked principle of NPR is similar to saturable absorber. The current experimental setup is schematically shown in Fig. 1. A segment of single-mode thulium-doped fiber (TDF, Nufern, SM-TSF-9/125) is used as gain medium, which is pumped by a 1565 nm erbium/ytterbium co-doped fiber laser through a 1570/2000 nm wavelength division multiplexer (WDM) [28]. The length, numerical aperture, mode field diameter, and cut-off wavelength of the TDF are 3 m, 0.15, 10.5 μm and 1700 $\pm$ 100 nm, respectively. TDF has an absorption coefficient of 13 dB/m at 1570 nm, and a dispersion parameter β_2 of $-0.0707\,\mathrm{ps}^2/\mathrm{m}$ at 1990 nm. Additionally, a segment of 50 m single-mode fiber (SMF) is spliced in the ring cavity to enhance the NPR effect. As a result, the mode-locked threshold can be decreased [29]. A 2 μm band optical isolator (ISO) is also employed in the cavity to ensure unidirectional operation. Except 3 m long TDF and 50 m long SMF, pigtails of the components in the cavity are all SMF. Dispersion parameter β_2 of SMF is $-0.0679\,\mathrm{ps}^2/\mathrm{m}$ at 1900 nm. The total cavity length is about 67 m including pigtails of components, and the net cavity dispersion is calculated to be $-4.4898\,\mathrm{ps}^2$ at 1900 nm. The output of ISO is connected to TDF and WDM, along with PC1, a 2 μm band polarizer and PC2.

The 90% port of the 90/10 optical coupler is engaged to feedback and the 10% port is output port. The output optical signal is divided by a 3 dB coupler, one portion is observed by an optical spectrum analyzer (YOKOGAWA, AQ6375) and the other is sent into an oscilloscope (Agilent, DSO-X 93204A) with 32 GHz bandwidth and 80 GSa sampling rate after a photodetector with 12 GHz bandwidth and 28 ps rising time.

$\alpha 1$ is the angle between the polarization direction of the input signal and the fast axis of the SMF, and $\alpha 2$ is the angle between the fast axis of the SMF and the polarization direction of the polarizer. Both $\alpha 1$ and $\alpha 2$ can be altered by adjusting the PC1 and PC2, respectively. The combination of PC-SMF-PC-polarizer acts as an intensity-dependent loss (IDL) [30], [31]. The NPR effect can be induced by two PCs and the polarizer in the cavity. The linearly polarized light can be formed by the polarizer, and then, it can be made elliptical polarized light by PC1. The state-of-polarization of the light rotates as it propagates in SMF due to *Kerr* effect. The angle of rotation is proportional to the light intensity. The signal passes through PC2 before arriving at the polarizer which allows only a certain polarization to pass through. By adjusting PC2, central part of the pulse can pass through the polarizer and the intensity of pulse wings can be suppressed, obviously, the intensity of the pulse center can be enhanced. As the pulse signals become narrower, the main nonlinear effects are self-phase modulation (SPM) and cross phase modulation (XPM). Stimulated Raman scattering (SRS) and self-frequency steepening, also acting as influence factors of pulse shape, make less effect in this configuration. Because these two effects are more sensitive to the pulses with short wavelength and high peak power, and it does not fit in with our experiment conditions.

In the experiment, maximum output power of the pump laser can be up to 2 W. Mode-locked threshold can be achieved when the pump power is increased to 800 mW, then we can observe *Kelly* sidebands of the mode-locked laser spectrum which is a typical feature of soliton, as shown in Fig. 2(a). The 3 dB bandwidth is about 4.7 nm. Another natural feature of soliton is the transform-limited sech^2-shaped pulse [32]. Obviously, the laser was operating in passively mode-locked state, and single pulse train is shown in Fig. 2(b). The pulse interval is 326.8 ns, corresponding to the repetition rate 3.06 MHz, and the repetition rate can be also calculated by the equation $f = c/nL$ [33], where

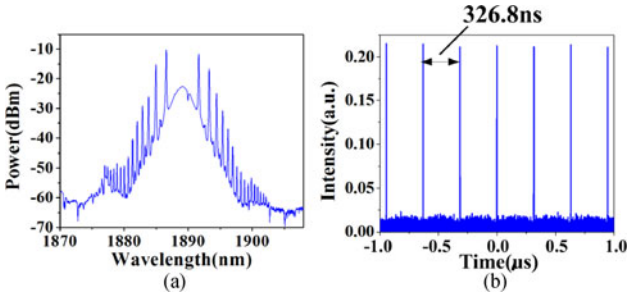

Fig. 2. (a) Output spectrum of mode-locked soliton pulse with Kelly sidebands. (b) Fundamental repetition rate pulse train obtained by NPR mode-locking.

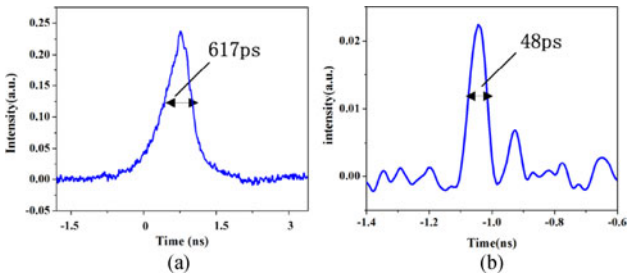

Fig. 3. (a) Single pulse time-domain waveform. (b) Compressed single pulse time-domain waveform.

c is the speed of the light, n is the refractive index of the fibers, L is the length of the ring cavity.

It is well known that fiber dispersion in the cavity is the main reason of laser pulse broadening. Therefore, in order to narrow the pulse width, a 4 m long dispersion compensation fiber (DCF) is used to compensate the dispersion. The pulse width can be compressed from 617 ps to 48 ps as shown in Fig. 3. After compression, the single pulse energy is 1.63 nJ and the peak power is about 34 W. The third-order dispersion compression can be ignored if the compressed pulse signal is more than dozens of picoseconds, and the oscillation at the tail of the compressed pulse signal has a negative effect on quality of the pulse signal presented by Qu *et al.* in [34].

B. High Repetition Rate Mode-Locked Fiber Laser

High repetition rate mode-locked fiber lasers have been intensively studied because of their numerous applications in metrology, spectroscopy and telecommunication [35], [36]. High repetition rate mode-locked pulse trains generation by harmonic mode-locking (HML) is considered to be effective. High-order HML pulse trains can be easily obtained by using passively mode-locked techniques.

HML can be understood as resulting from a weak repulsive force attributed to the gain medium depletion and the recovery time between subsequent solitons [37]. For the experimental setup as Fig. 1, if we continue increasing the pump power, the mono-pulse signal can be divided into multi-pulse signals, and then high-order harmonic mode-locked pulse train can be formed.

Further reduction of the pulse width is limited due to the generation of soliton sideband spectrum. In the steady state, whether the peak power of soliton reaches the maximum value is

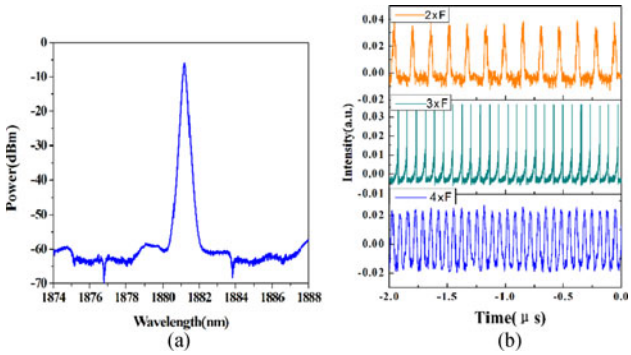

Fig. 4. (a) Harmonic mode-locked spectrum. (b) Harmonic mode-locked pulse train. F: fundamental frequency.

determined by the saturated additive pulse mode-locking (APM). Since the mode-locked soliton pulse energy has quantum effect, the optical pulse energy of soliton in fiber ring cavity cannot be rising continuously with the increasing of the pump power. Therefore, it results in multi-soliton oscillations in the cavity on the contrary. Also, there are mutual repulsion interactions between the solitons, as a result, high-order harmonic mode-locked pulse trains can be observed. The NPR effect can reach saturation when the pump power continues increasing, the transmission degrades with further enhancing of light intensity, and multi-wavelength output can be observed because of the intensity-dependent loss induced by NPR effect.

In the process of high-order harmonic mode-locked pulse train, the fundamental frequency mode-locked pulse train is formed firstly, and then a mono-pulse signal split into multi-pulse signals. Finally, high-order harmonic mode-locked pulse train can be formed. In the experiment, the spectrum of harmonic mode-locked pulse sequence is shown in Fig. 4(a) and the 3 dB bandwidth is about 0.3 nm, which is much narrower than Fig. 2(a) and other conventional soliton such as [32] and [38]. In the experiment, the spectrum bandwidth is always narrower when the number of HML increases. Because passive mode-locked fiber laser with narrower spectrum bandwidth or narrower additional filtering bandwidth has stronger ability to hold a multi-pulse state. The related theoretical and experimental models have been verified by using additional filtering method [39]. As a result of spectrum bandwidth becoming narrower, the Kelly sidebands become weaker even disappear. Similar results are also proposed in [40]. The pulse amplitude can be observed by an oscilloscope and the harmonic mode-locked pulse train is shown in Fig. 4(b).

Then high-order harmonic mode-locked pulse trains are formed by different methods, and the repetition rate is integer times of fundamental frequency. In addition, with further increasing of pump power, the pulses of the output laser perform complex transformation while adjusting PCs.

The passively mode-locked fiber lasers can adopt combination of two mechanisms to enhance the repetition rate [41]–[44]. Semiconductor saturable absorption mirror (SESAM) is an excellent mode-locked device for fiber lasers, its mode-locked mechanism uses mainly intensity-dependent loss to narrow the pulses [45]. Then, in the following experiment, a SESAM is connected into the ring cavity by an optical circulator between

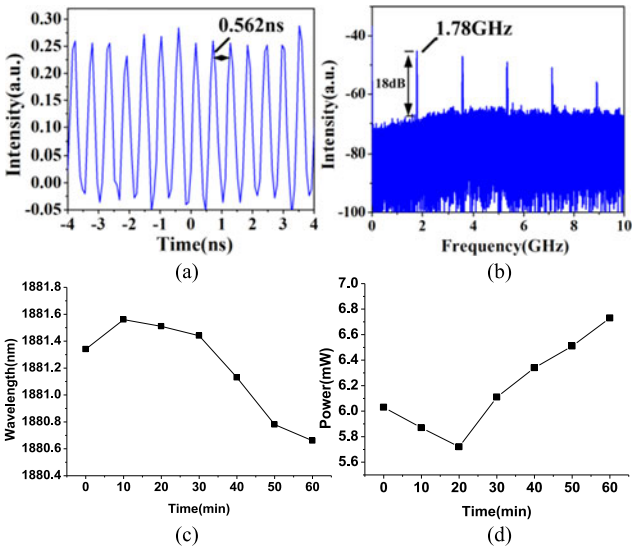

Fig. 5. (a) 1.78 GHz HML pulse train. (b) RF spectrum of HML pulse train obtained by hybrid mode-locked. (c) Wavelength drift. (d) Power fluctuation.

the coupler and SMF in Fig. 1. The modulation depth, the recovery time and the saturation fluence of SESAM are 1.2%, 30 ps, and 70 μJ/cm^2, respectively. Peak of pulses can pass through SESAM with low loss while wings are cut off due to higher loss. Therefore, pulses can be narrowed to generate mode-locked pulse trains.

Since there are two mode-locked mechanisms in the laser, pulses experience twice amplitude modulation per round trip, though which, the pulse wings are cut down more effectively than single mode-locked mechanism, then the width of pulses become narrower. While slowly increasing the pump power in the experiment, the high-order harmonic increases stepwise as the pump power increases. The passive HML can keep operating stably. In the experiment, the maximum repetition rate is 1.78 GHz corresponding to 588th-order HML pulse train with 1 W pump power, the time domain waveform and radio frequency (RF) spectrum are observed in Fig. 5(a) and (b). The pulse interval is 0.562 ns corresponding to 588 times of cavity round-trip-time. The supermode suppression ratio is about 18 dB. Fig. 5(c) and (d) show the wavelength drift and the power fluctuation in 60 min, i.e., $\pm$0.49 nm and $\pm$0.5 mW respectively. Therefore, we believe that it can be acceptable for a GHz level mode-locked fiber laser without any external stability mechanism. Neither multi-wavelength output nor pulse split is appeared, indicating that SESAM plays a leading role in the generation of mode-locking, and NPR is mainly used for pulse shaping and enhancement of nonlinear effects. In the experiment, we do not observe the split of wavelength and pulse because the intensity dependent loss induced by NPR can suppress the mode competition and guarantee the stable HML operation [46]–[48]. In order to prevent the damage of SESAM, the pump power cannot be increased continuously. Therefore, we cannot observe higher order (higher than 588th-order) harmonic pulse in this experiment.

In the experiment, we found that repetition rate can be adjusted by increasing pump power or polarization state in the cavity. In fact, the repetition rate of the pulse is mainly affected by the ellipticity of mode-locked fiber lasers [49]. By increasing the pump power in conjunction with minor adjustments to the PCs, resulting in a wider ellipticity range can accommodate mode-locked operation [50]. Therefore, high-order HML pulse trains are obtained by both increasing the pump power and adjusting the PCs.

C. Widely Tunable Mode-Locked Fiber Laser

Both TDF and HDF have a quite wide spontaneous emission band, which has the obvious advantage to achieve widely tunable lasers in 2 μm region. It is of great use especially in free-space optical communications due to its high transmissivity and insensitive character to Rayleigh scattering. It is also more convenient and cost-effective comparing to using multiple lasers with different operating wavelengths. The tunable mode-locked fiber laser, to be a new research direction, has been studied recently. In previous works, a tunable pulse ytterbium-doped fiber laser is obtained, through fabricating a few-layer molybdenum disulfide (MoS_2) polymer composite saturable absorber and a tunable band-pass filter [51]. A 75 nm tunable mode-locked state around 1550 nm based on a variable attenuator and NPR effect to control the intra-cavity loss was reported [52]. NPR effect can induce wavelength or intensity dependent loss of the cavity to alleviate the mode competition caused by the homogeneous gain broadening [14], [53]. Liu *et al.* demonstrate a bandwidth and wavelength-tunable fiber laser with an intracavity FBG. Even more, the pulse width can be accurately tuned from 7 to 150 ps in this novel configuration [40]. However, these researches are more concentrated on 1 μm and 1.5 μm band. Yan *et al.* demonstrate widely tunable Tm-doped mode-locked fiber lasers and it verifies that nonlinear polarization evolution (NPE) effect is an effective technique to achieve widely mode-locked fiber laser at 2 μm band [20], [21].

In the experimental setup of Fig. 1, a segment of 3.1 m polarization maintaining fiber (PMF) is inserted between the polarizer and PC1 [54]. Therefore, a birefringence Lyot filter can be consisted of PMF, polarizer and PC1. In order to obtain wider gain region, a 7 m long TDF is introduced in this experiment. Including the pigtails, the total cavity length is about 65 m. Birefringence Lyot filter, as a comb filter, can be effectively used to expand the tuning range of mode-locked fiber laser [55], [56].

The tunability of pulsing lasers results from the NPR structure combining with two PCs, polarizer and pigtails of components. When the light propagates through the polarizer, linearly polarized light is formed. The angle between polarization direction of the light and the fast axis of the pigtails comes to $\alpha 1$ as light pass through PC1, and it alters to $\alpha 2$ as the light spreads along fibers to PC2 due to the *Kerr* effect. Adjusting angles of PC1 and PC2, $\alpha 1$ and $\alpha 2$ can be modified, so the loss of cavity can be changed. The power transmission of the cavity is given by [57]

$$T = \cos^2\alpha_1 \cos^2\alpha_2 + \sin^2\alpha_1 \sin^2\alpha_2 + \frac{1}{2}\sin 2\alpha_1 \sin 2\alpha_2 \cos\left(\Delta\Phi_L + \Delta\Phi_{NL}\right) \quad (1)$$

here, $\Delta\Phi_L$ and $\Delta\Phi_{NL}$ are linear and nonlinear phase shift between the polarization components, respectively, and they

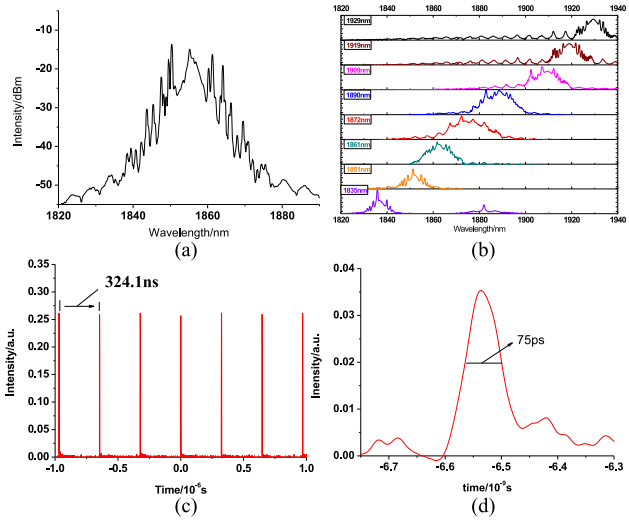

Fig. 6 (a) Mode-locked spectrum. (b) Tunable single-wavelength mode-locked spectrum from 1835 nm to 1929 nm. (c) Pulse repetition rate of single wavelength mode-locked output. (d) FWHM of single pulse.

can be expressed as

$$\Delta\Phi_L = 2\pi L(n_y - n_x)/\lambda \tag{2}$$

$$\Delta\Phi_{NL} = 2\pi n_2 PL\cos(2\alpha_1)/\lambda A_{\text{eff}} \tag{3}$$

where n_x and n_y are refractive indices of fast and slow axes of the birefringence fiber, respectively. *L* is the length of the birefringence fiber. In the proposed fiber cavity, the birefringence fiber consists of a SMF, pigtails of fiber components and a PMF in the *Lyot* filter. λ is the operating wavelength, n_2 is the nonlinear (*Kerr*) coefficient, *P* is the instantaneous power of light, and A_{eff} is the effective fiber core area. In the equals, the peak transmission can reach 100% when $\alpha 1$ and $\alpha 2$ are orthogonal. SPM and XPM in cavity can cause phase shift of two orthogonal polarization lights. The phase shift causes intensity modulation on the cavity net gain. Stable mode-locking can occur at a particular wavelength in gain bandwidth of TDF under orthogonal condition. If the angle between $\alpha 1$ and $\alpha 2$ is offset from 90°, the mode-locking still exists but it becomes less stable with some continuous-wave components. NPR can cause the variation of intensity dependent loss at different wavelengths. This inhomogeneous loss can be used to alleviate the mode competition induced by the homogeneous gain broadening of TDF and realize tunable operation at both continuous-wave and mode-locked state. The threshold of the mode-locked state is higher than that of the continuous-wave state. Consequently, output spectrum of the mode-locked pulse can be tuned by adjusting PCs to above the mode-locked threshold.

Fixing pump power at 1 W, the laser can reach mode-locked threshold. Further increasing pump power to 1.5 W, output spectrum broadens with about 20 nm full width at half maximum (FWHM), and it is observed through an OSA with the resolution of 0.05 nm as shown in Fig. 6(a). The spectrum presents *Kelly* sidebands abundantly, which is the representative characteristic of soliton in anomalous dispersion fiber lasers [58]. By adjusting PCs attentively, the tunable mode-locked spectrum can be observed, with center wavelength from 1835 nm to 1929 nm, as shown in Fig. 6(b). As we know the tuning effect is resulted from the inhomogeneous loss in the cavity by adjusting PCs. The *Lyot* filter consisting of a PC and PMF can expend tuning range because the comb filtering can reduce the self-start threshold of continuous and mode-locked state. Therefore the laser can oscillate at sideband of the ASE spectrum (1820–1840 nm and 1920–1940 nm). The intensity and bandwidth of spectrum reach maximum at about 1870–1890 nm during the tuning process. It is resulted from the uneven gain spectrum of TDF. Mode-locked state around center wavelength tends to achieve higher intensity and wider bandwidth. Fig. 6(c) shows that the pulse interval is 324.1 ns corresponding to the repetition rate 3.085 MHz which is determined by the totally cavity length of 65 m. The pulse width seems broader comparing with NPR based passively mode-locked fiber laser pulses in 1.55 μm and 1 μm region. It is attributed to the strong anomalous dispersion of the SMF for 2 μm band. The mode-locked laser pulses can be compressed through administrating the net dispersion with dispersion compensating components. Pulse width of the tunable mode-locked fiber laser is about 75 ps measured by an oscilloscope through a photo detector with the bandwidth of 10 GHz in Fig. 8(d).

III. Mode-Locked Tm/Ho-Co Doped Fiber Laser Based on NALM

Nonlinear amplifying loop mirror is a straight forward extension of the nonlinear optical loop mirror (NOLM) and it can improve the mode-locked fiber laser apparently due to its saturable absorption and fast switching. Theoretically, NALM structure can output femtosecond pulse [59], [60]. Recent years, NALM passively mode-locking technology has been widely used in ultra-short pulse fiber lasers. In the past decade, high power pulse fiber lasers have been gradually improved by NALM structure and the popularity of all-fiber lasers. NALM structure can produce new high power dissipative pulse laser types such as dissipative soliton resonance (DSR) [61]–[63] and rectangular noise-like pulse (NLP) [64]–[66]. The high energy dissipation pulse with NALM structure relies heavily on the combined effect of laser gain, loss, dispersion and fiber nonlinearity. It should be noted that there is no polarization discrimination component in NALM structure. Thus, a variety of vector pulses can be observed in NALM mode-locked fiber laser according to references [67], [68].

Mode-locked fiber lasers based on NALM in 1 μm and 1.55 μm region are often reported, just as our research work about square-wave pulse at 1.55 μm [69]. However, mode-locked square-wave pulse fiber lasers at 2 μm band with NALM are seldom reported. Therefore, we have been studying mode-locked fiber lasers based on NALM recently. In this section, we would like to demonstrate our recent research works about the square-wave mode-locked fiber laser at 2 μm band and its characteristics.

A. Experimental Setup and Principle

The basic mode-locked fiber laser based on NALM structure is shown in Fig. 7. In this experimentally setup, a segment of 4 m long thulium/holmium co-doped fiber (THDF, INO,

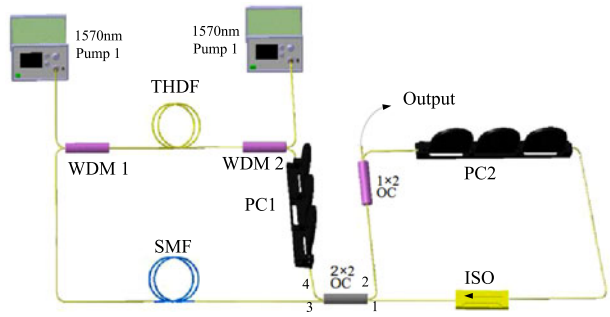

Fig. 7. Configuration of mode-locked thulium/holmium co-doped fiber laser based on NALM. THDF: thulium/holmium co-doped fiber; OC: optical coupler.

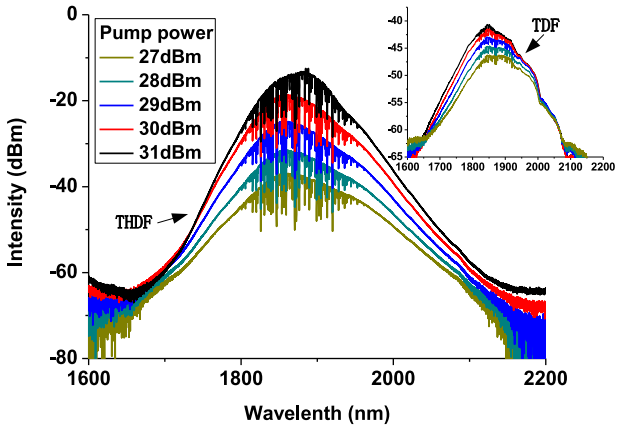

Fig. 8. Amplified spontaneous emission (ASE) of the THDF and TDF pumped by 1570 nm laser with different pump power. Inset: ASE of the TDF under the same pump condition with THDF.

TH-540) pumped bidirectionally by two fiber lasers operating at 1570 nm through two 1570/2000 nm WDMs is spliced into a fiber loop. Obviously, a typical thulium/holmium co-doped fiber amplifier (THDFA) can be constructed.

As shown, NALM consists of the THDFA, a PC (PC1) and a 30 m SMF used to improve nonlinear effects. A unidirectional fiber loop (UL) including an ISO and a PC (PC2) connects the NALM by a 50/50 optical coupler. A 10/90 optical coupler is used as output coupler, and 10% power is output meanwhile 90% power is feedback. The ISO can ensure that the light transmits in single direction in UL, and PC1 and PC2 can be used to adjust the polarization state in NALM and UL respectively.

Total length of the intra-cavity fiber is about 46 m including SMF, THDF, fiber devices and their pigtails. Both SMF and THDF in the experiment are negative dispersion fiber at 2 μm band, therefore, the laser can operate in a strong negative dispersion region. The output laser can be observed by an optical spectrum analyzer for the output spectrum and the pulse sequence in time domain can be observed by an oscilloscope with a photo detector.

In the experiment, the numerical aperture (*NA*) and cut-off wavelength of the THDF are 0.019 and 1800 nm, respectively. THDF has an absorption coefficient of 85 dB/m at 1570 nm. As we know, longer wavelengths optical gain at 2 μm band can be generated because THDF has higher pump efficiency than TDF. Fig. 8 shows the amplified spontaneous emission (ASE) of 4 m long THDF, and the insert figure shows ASE spectrum of 4 m

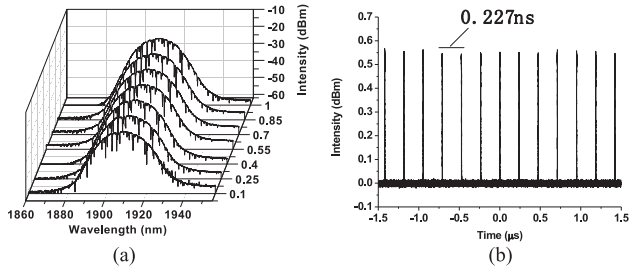

Fig. 9. (a) Mode-locked spectrum of fiber laser based on NALM. (b) Oscilloscope trace of mode-locked pulse sequence.

long TDF. In the experiment, we use the same pump powers, obviously, the emission wavelength can be extended to longer band and the pump efficiency can be improved due to higher absorption efficiency of the THDF comparing with the TDF.

With low input power of NALM, it operates in the linear regime, and a pulse coupled in at port1 is reflected and amplified back to port1. No light emerges from port2. Since the THDFA is placed at one end of the loop, the nonlinear refractive index n_2 leads to a change in the optical path lengths for light propagating clockwise and counter clockwise around the loop at high optical input power and to phase changes of $\delta\phi_c$ and $\delta\phi_{cc}$, respectively. If the THDFA and the pulse lengths are shortly compared with the total loop length, and the individual pulse does not saturate the amplifier, the phase delays can be given by [70]

$$\delta\phi_c = \frac{\pi}{\lambda_s} n_2 g I_{s0} L \tag{4}$$

$$\delta\phi_{cc} = \frac{\pi}{\lambda_s} n_2 I_{s0} L \tag{5}$$

where I_{s0} is the signal intensity launched into port1, L is the fiber length, λ_s is the signal wavelength, and g is the gain of the THDFA. The reflectivity and transmittance of NALM can be expressed respectively by the transfer matrix method

$$R = \frac{1}{2}[1 + \cos(\delta\varphi_c - \delta\varphi_{cc})] \tag{6}$$

$$T = \frac{1}{2}[1 - \cos(\delta\varphi_c - \delta\varphi_{cc})] \tag{7}$$

Therefore, according to the transmission characteristics, transmissivity of the NALM can be enhanced with the increasing of the incident light power, and reflectivity can be decreased with the increasing of the incident optical power. Obviously, NALM is a fast optical switch similar to the saturable absorber, called like-absorber, and it can be used as an ultrafast mode-locked device in fiber laser.

B. Noise-Like Square-Wave Pulses at 2 μm Band

Firstly, in the experiment, power of pump1 is enhanced gradually without pump2. When power of pump1 reaches 1 W, mode-locked self-starting condition can be met due to the generation of the saturable absorption effect in NALM. The output broadband spectrum of the mode-locked fiber laser at 2 μm band is shown in Fig. 9(a), the 3 dB bandwidth can be broadened to 15 nm. As we know, the output spectrum of a typical mode-locked soliton pulse must have *Kelly* sideband at the center peak wavelength. However, it is easy to see that the mode-locked pulse spectrum is

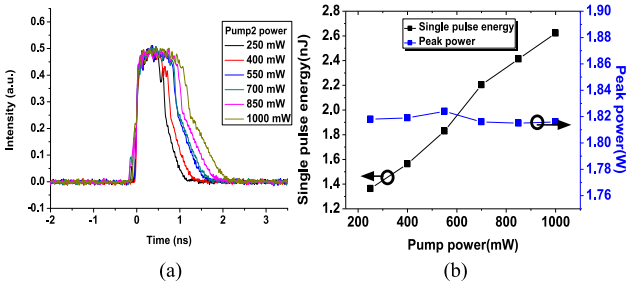

Fig. 10. Details of square-wave pulse at 2 μm band with the pump2 from 250 mW to 1W. (a) Waveform. (b) Single pulse energy and peak power.

very smooth, and we cannot observe any modulation sidebands in spectrum of the mode-locked pulse laser. The smoother and broader spectrum is the typical spectral characteristic of noise-like pulse (NLP) [71] as shown in Fig. 9(a). Obviously, this mode-locked laser pulse is a kind of NLP according to [72].

As we know, generation of NLP in the mode-locked fiber laser needs higher pump power, therefore, normally it is difficult to observe NLP fiber lasers in 2 μm region. In the experiment, due to higher pump efficiency of the THDF, NLP can be observed at 2 W pump power. Fig. 9(b) shows the pulse sequence of mode-locked fiber laser, the amplitude is balanced and round trip time of the cavity is 0.227 ns corresponding to the 4.4 MHz repetition rate.

Fig. 10(a) shows details of the mode-locked laser pulse at 2 μm band, and the shape of the pulse is approximately square-wave. Then, power of pump2 is increased from 250 mW to 1 W, and meanwhile, the pulse width in time domain can be extended from 0.75 ns to 1.3 ns. Fig. 10(b) shows the variations of single pulse energy and peak power. The single pulse energy changes from 1.363 to 2.622 nJ with pump2 power increasing from 250 to 1000 mW. However, peak power of the pulse is always around 1.82 W and cannot be changed with the increasing of the pump power. Although the top of this waveform cannot be as flat as the square-wave pulse in our previous work in 1.55 μm region [69], we can conclude that it must be a real square-wave pulse at 2 μm band.

In our previous report on mode-locked fiber lasers at 1.55 μm band, a square-wave noise-like pulse with pulse width of 1.5 ns can be observed [69], and the back edges of the pulse is steeper than the square-wave pulse in this experiment. As we know, the back edge of the pulse is mainly composed of red shift components (longer wavelength) in fiber, and the fiber has a larger negative dispersion in 2 μm region than in 1.55 μm region. Therefore, the propagation velocity of red shift components in 2 μm fiber system is slower than that in 1.55 μm system. Obviously, the square-wave pulse in 1.55 μm mode-locked fiber laser has a steeper back edge.

Square-wave NLP has been reported in the study of mode-locked erbium-doped fiber laser (EDFL) at 1.55 μm band for the last three years, and it is the first time to our knowledge that square-wave NLP in 2 μm region is observed.

Frequency spectrum of the square-wave mode-locked pulse is shown in Fig. 11. The frequency spectrum is recorder from 0 to 50 MHz with the resolution of 200 kHz. The repetition rate of mode-locked is 4.4 MHz corresponding to the cavity length of

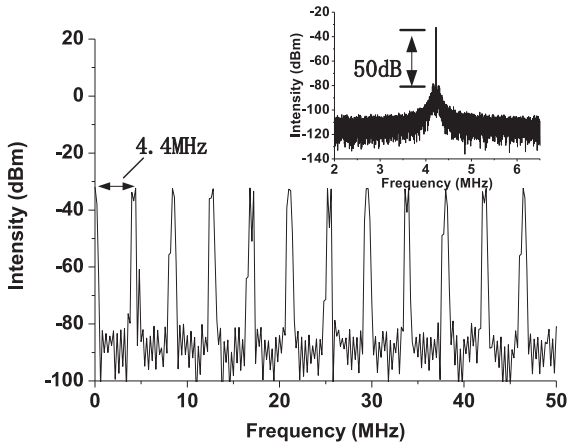

Fig. 11. Corresponding RF spectrum. Inset: Fundamental frequency RF spectrum.

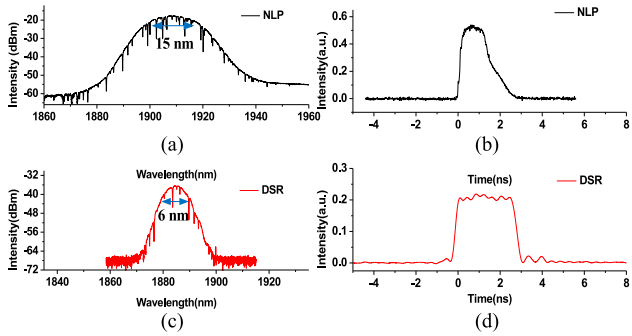

Fig. 12. Differences between square-wave NLP and DSR. (a) Spectrum of NLP. (b) Pulse profile of NLP. (c) Spectrum of DSR. (d) Pulse profile of DSR.

46 m. In addition, details of the fundamental frequency spectrum are also shown in the inset figure with the resolution of 1 Hz. More additional structure can be revealed with high resolution and the side-mode suppression ratio (SMSR) is about 50 dB in frequency range of 6.5 MHz and no sideband appears. Therefore, we can conclude that noise of laser is relatively low.

As we know the specific autocorrelation trace with a spike on each scanning curve is a common feature to judge the NLPs. Here we cannot provide the autocorrelation trace, limited by our experimental conditions. However we can judge the square NLPs from the profiles of spectrum and pulse. The 3 dB spectrum in our experiment reaches 15 nm, as shown in Fig. 12(a). For a conventional soliton pulse or DSR, such broad spectrum bandwidth corresponds to hundreds or even dozens of fs pulse width and it is impossible to be achieved in an all fiber 2 μm band fiber laser with 44 m long cavity without any compression mechanism, as silica fiber has a much strong negative dispersion than 1.55 μm. The NLPs are formed by discrete multiple ultrashort pulses with ultra broad spectrum in a large number previous reports. The unsmooth top and slanted back edge also show the discrete distribution characteristics of NLPs, as shown in Fig. 12(b). Actually, the squae-wave NLPs and DSRs can be transformed from each other by carefully adjusting the PCs in our experiment. The specific spectrums and pulse shapes are shown in Fig. 12(c) and (d). The 3 dB spectrum bandwidth of DSR is only 6nm and the DSR has a much steeper back edge,

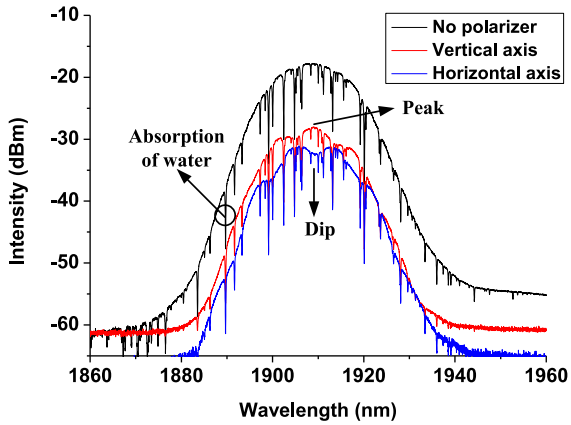

Fig. 13. Vector pulse emission fiber laser spectrum. Black line: the total laser emission without passing through a polarizer. Red and Blue lines: the two orthogonal polarization components resolved with an external cavity polarization beam splitter.

which are the main differences between the NLPs. In this paper we only focus on the NLPs and more detailed analysis on DSRs will be discussed in our following report.

In order to further observe the vector characteristics of the square-wave NLP, we connect a polarization beam splitter (PBS) at the output port to analyze pulse states of two orthogonal polarization directions of the square-wave pulse. A polarization controller is inserted between the output port and the polarization beam splitter in order to balance the fiber pigtail induced linear polarization rotation. The polarization resolved spectrums of the square-wave pulse are shown in Fig. 13. It can be seen that the spectrum bandwidth of the two orthogonal polarization components is almost unchanged and the intensity decreases after PBS in comparison with the output pulse spectrum without polarizer.

On the polarization resolved spectrum, there are peaks, the other set of spectrum displays neither as a peak or a dip, between the two orthogonal polarization components there is always a peak-dip relationship. When the PCs in the cavity are adjusted, the intensity of the peak and dip are slightly varied and the relationship cannot be broken, indicating the existence of coherent energy exchange [73]. Additionally, there are dips in all the three lines much deeper and narrower, the dips always locate at the same wavelength and the depth hardly changes when adjusting the PCs. We deduce that the deeper dips are caused by the absorption of water. Time-domain pulse traces of the two orthogonal polarization components are presented in Fig. 14. They have uniform and equal pulse amplitudes. Being different from the polarization rotation vector pulse, the obtained pulses have exactly the same polarization and it can remain unchanged during propagation in the cavity. The results can prove that the square-wave pulse has typical polarization-locked vector characteristics [74].

C. Square-Wave Noise-Like Pulses With Multi-Pulse

When two pump powers are all at 1 W, a kind of square-wave noise-like pulse with low intensity pulse bunches can be observed by adjusting PC1 in the experiment, and the

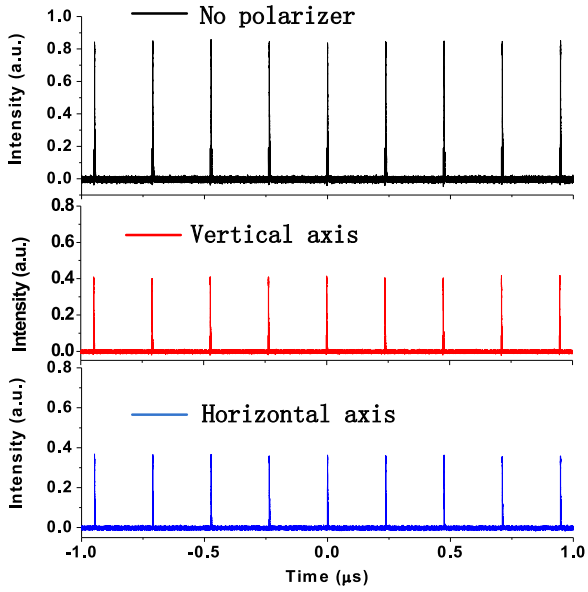

Fig. 14. Oscilloscope traces of the pulse train in a polarization-locked vector pulse operation state. Black line: the total laser emission without passing through a polarizer. Red and Blue lines: the two orthogonal polarization components resolved with an external cavity polarization beam splitter.

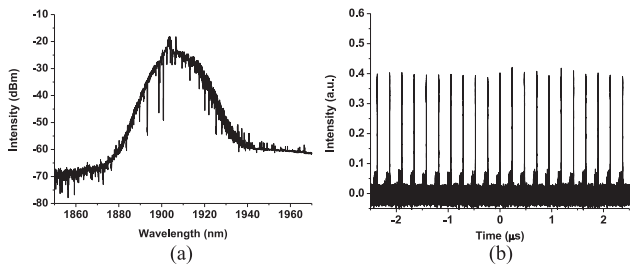

(a) (b)

Fig. 15. (a) Mode-locked spectrum of fiber laser with multi-pulse. (b) Oscilloscope trace of mode-locked pulse sequence.

measurement spectrum is shown in Fig. 15(a). We can observe typical wideband spectrum of square-wave noise-like pulses without any sideband components, but some irregular burrs on the spectrum can also be found. Fig. 15(b) shows the pulse sequence of time domain measured by an oscilloscope, obviously, the interval of the pulses can maintain 0.227 ns. However, in each round trip time, there are a series of lower intensity pulse bunches adjacent to the left side of mode-locked square-wave pulses. These pulse bunches only occupy a small part of resonant round trip time in the time domain.

Fig. 16 shows the details of a single square-wave pulse and its following pulse bunches in time domain observed by an oscilloscope with the sample rate of 100 GSa/s. These low intensity pulse bunches are comprised of a large number of randomly distributed bound pulses, and they are accompanied by the mode-locked noise-like pulse signal. Therefore, we can conclude that these low intensity pulse bunches are operating at multi-pulse mode-locked state with high pump power, and the repetition rate is just corresponded to the repetition rate of the mode-locked fiber laser. The generation of these multi-pulse bunches is resulted from nonlinear effects in the fiber under the condition of high pump power.

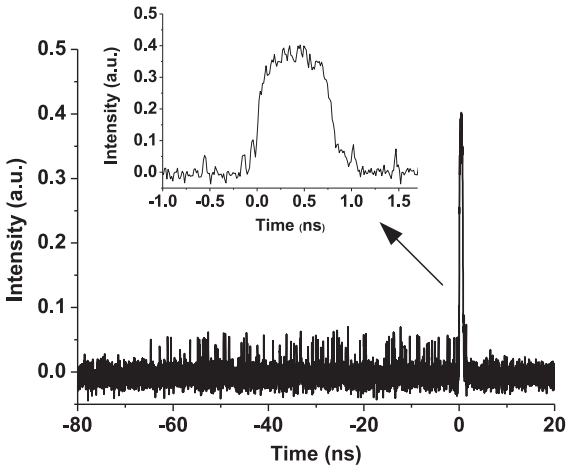

Fig. 16. Details of square-wave pulse with multi-pulse.

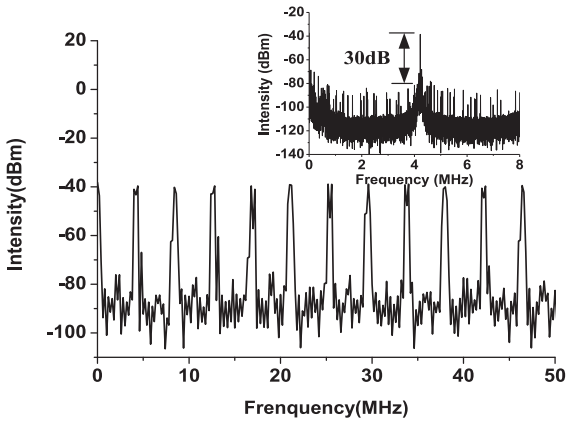

Fig. 17. RF spectrum of the square-wave mode-locked pulse with multi-pulse bunches. Inset: RF spectrum of the fundamental frequency.

However, the width of square-wave pulse is narrowed from 1.3 ns to 0.8 ns compared with Fig. 10 because the energy of square-wave pulses is clamped by the multi-pulse bunches. As we know, since the pulse bunches comprise several tens of pulses and they have intra-cavity interactions, these mode-locked multi-pulse belong to the category of multi-pulsing dynamics. Multi-pulsing is the typical result of conjunction of a relatively strong pumping power with propagation in an anomalous dispersive cavity. Intra-cavity pulses have erratic relative motions, stabilize themselves at more or less random relative positions, or distribute themselves regularly all along the cavity [75]. These multi-pulse bunching is corresponding to the ability of several identical pulses to group themselves in a stable and tight packet whose duration is much shorter than the cavity round-trip time [76], [77].

Fig. 17 shows the corresponding frequency spectrum with the resolution of 200 kHz, and the repetition rate of the mode-locked NLP is still 4.4 MHz. Detail of the fundamental frequency spectrum is also shown in the inset of figure with the resolution of 1 Hz. We can see a large numbers of side-modes on both sides of the center frequency, the SMSR is only 30 dB. The side modes correspond to the frequency components of many low intensity bound pulses, multi-pulse bunches, indicating that these pulses have different group velocities. This characteristic can also be shown by the property of the optical spectrum and the irregular burrs on the spectrum as shown in Fig. 14(a).

Based on experimental results, we can conclude that the dynamics of the square-wave NLP with low intensity multi-pulse bunches can be understood as an intermediate regime similar to a soliton rain [78]. In this intermediate regime, mode-locked square-wave NLPs and continuous wave (CW) components of comparable strength not only coexist but also interact in a dramatic way [79]. With higher pump power, new pulses form from a noisy background spontaneously. The existence of a CW component is also known to mediate interactions between pulses, thus strongly affecting multi-pulsing dynamics [80]–[82]. At high pump power, mode-locking is readily associated with multi-pulsing. We refer to this intermediate regime as one of weak mode-locking, since low-intensity waves cannot be as efficiently filtered out as they are in usual mode-locking. This intriguing finding in our experiment, we intend to investigate in depth through future experiments.

IV. Conclusion

In conclusion, we introduced mode-locked fiber lasers operating at 2 μm band based on NPR in previous research work and NALM in recent research work. We also introduced the current state of passively mode-locked fiber lasers at 2 μm band. In our experiments of thulium-doped fiber lasers based on NPR, high repetition rate of 1.78 GHz with combination of HML and SESAM, and mode-locked pulse tuning range of 94 nm can be observed. In this paper, a square-wave NLP at 2 μm band based on NALM and a kind of square-wave mode-locked pulse with low intensity multi-pulse bunches are observed and analyzed. Mode-locked fiber lasers at 2 μm band have many potential applications in radar, remote sensing, and free-space optical communications. Future work will include further study of the mode-locked pulse compression in 2 μm region.

References

[1] B. Richards, Y. Tsang, D. Binks, J. Lousteau, and A. Jha, "Efficient 2 μm Tm^{3+}-doped telluride fiber laser," *Opt. Lett.*, vol. 33, pp. 402–404, 2008.

[2] N. J. Scott, C. M. Cilip, and N. M. Fried, "Thulium fiber laser ablation of urinary stones through small-core optical fibers," *IEEE J. Sel. Top. Quantum Electron.*, vol. 15, no. 2, pp. 435–440, Mar./Apr. 2009.

[3] M. Eckerle *et al.*, "Actively Q-switched and mode-locked Tm^{3+}-doped silicate 2 μm fiber laser for supercontinuum generation in fluoride fiber," *Opt. Lett.*, vol. 37, pp. 512–514, 2012.

[4] C. R. Phillips *et al.*, "Supercontinuum generation in quasi-phase-matched $LiNbO_3$ waveguide pumped by a Tm-doped fiber laser system," *Opt. Lett.*, vol. 36, pp. 3912–3914, 2011.

[5] P. Zhang, T. Wang, W. Ma, K. Dong, and H. Jiang, "Tunable multi-wavelength Tm-doped fiber laser based on the multimode interference effect," *Appl. Opt.*, vol. 54, pp. 4667–4671, 2015.

[6] Z. Lou *et al.*, "Grapheme mode-locked and Q-switched 2-μm Tm/Ho co-doped fiber lasers using 1212-nm high-efficient pumping," *Opt. Eng.*, vol. 55, 2016, Art. no. 080310.

[7] W. Zhou, D. Shen, Y. Wang, H. Ma, and F. Wang, "A stable polarization switching laser from a bidirectional passively mode-locked thulium-doped fiber oscillator," *Opt. Express*, vol. 21, pp. 8945–8952, 2013.

[8] M. Currie *et al.*, "Mode-locked 2 μm wavelength fiber laser using a grapheme-saturable absorber," *Opt. Eng.*, vol. 52, 2013, Art. no. 076101.

[9] J. Li *et al.*, "All-fiber passively mode-locked Tm-doped NOLM-based oscillator operating at 2-μm in both soliton and noisy-pulse regimes," *Opt. Express*, vol. 22, pp. 7875–7882, 2014.

[10] Z. Yang, Z. Yu, X. Zhang, and Y. Song, "Numerical analysis of the nonlinear polarization rotation mode-locked pulses in fiber," in *Proc. SPIE*, 2011, vol. 83071, pp. 1–6, Art. no. 83071Q.

[11] X. Wang *et al.*, "Tunable, multi-wavelength Tm-doped fiber laser based on polarization rotation and four-wave mixing effect," *Opt. Express*, vol. 21, pp. 25977–25984, 2013.

[12] X. Wang, P. Zhou, X. Wang, H. Xiao, and Z. Liu, "Pulse bundles and passive harmonic mode-locked pulses in Tm-doped fiber laser based on nonlinear polarization rotation," *Opt. Express*, vol. 22, pp. 6147–6153, 2014.

[13] J Li *et al.*, "Thulium-doped all-fiber mode-locked laser based on NPR and 45°-tilted fiber grating," *Opt. Express*, vol. 22, pp. 31020–31028, 2014.

[14] S. Liu *et al.*, "A multi-wavelength thulium-doped silica fiber laser incorporating a highly nonlinear fiber," *J. Opt.*, vol. 16, pp. 1–5, 2014.

[15] P. Liu *et al.*, "Widely tunable multi-wavelength thulium-doped fiber laser based on nonlinear polarization rotation," *Microw. Opt. Technol. Lett.*, vol. 58, pp. 1540–1543, 2016.

[16] M. Zhang *et al.*, "Tm-doped fiber laser mode-locked by graphene-polymer composite," *Opt. Express*, vol. 20, pp. 25077–25084, 2012.

[17] R. Gumenyuk, I. Vartiainen, H. Tuovinen, and O. G. Okhotnikov, "Dissipative dispersion-managed soliton 2 μm thulium/holmium fiber laser," *Opt. Lett.*, vol. 36, pp. 609–611, 2011.

[18] A. Hemming *et al.*, "High power operation of cladding pumped holmium-doped silica fiber lasers," *Opt. Express*, vol. 21, pp. 4560–4566, 2013.

[19] V. J. Matas, T. P. Newson, D. J. Richardson, and D. N. Payne, "Self-starting passively mode-locked fiber ring soliton laser exploiting nonlinear polarization rotation," *Opt. Commun.*, vol. 28, pp. 1391–1393, 1992.

[20] Z. Yan, B. Sun and X. Li, "Widely tunable Tm-doped mode-locked all-fiber laser," *Sci. Rep.*, vol. 6, 2016, Art. no. 27245.

[21] Z. Yan, X. Li and Y. Tang, "Tunable and switchable dual-wavelength Tm-doped mode-locked fiber laser by nonlinear polarization evolution," *Opt. Express*, vol. 23, pp. 4369–4376, 2015.

[22] D. Yan, X. Li, and S. Zhang, "L-band wavelength-tunable dissipative soliton fiber laser," *Opt. Express*, vol. 24, pp. 739–748, 2016.

[23] Z. Cheng, H. Li, and Pu Wang, "Simulation of generation of dissipative soliton, dissipative soliton resonance and noise-like pulse in Yb-doped mode-locked fiber lasers," *Opt. Express*, vol. 23, pp. 5972–5981, 2015.

[24] X. He, L. Hou and M. Li, "Bound states of dissipative solitons in the single-mode Yb-doped fiber laser," *IEEE Photon. J.*, vol. 8, no. 2, 2016, Art. no. 1500706.

[25] Z. Wu, S. Fu, and Kai Jiang, "Switchable thulium-doped fiber laser from polarization rotation vector to scalar soliton," *Sci. Rep.*, vol. 6, 2016, Art. no. 34844.

[26] C. Lecaplain and P. Grelu, "Multi-gigahertz repetition-rate-selectable passive harmonic mode locked of a fiber laser," *Opt. Express*, vol. 21, pp. 10896–10902, 2013.

[27] G. J. Cowle and D. Y. Stepanov, "Hybrid Brillouin/erbium fiber laser," *Opt. Lett.*, vol. 21, pp. 1250–1252, 1996.

[28] Q. Jia *et al.*, "Passively harmonic mode-locked pulses in thulium-doped fiber laser based on nonlinear polarization rotation," *Opt. Eng.*, vol. 55, 2016, Art. no. 106121.

[29] X. Feng, H.-Y. Tam, and P. K. A. Wai, "Stable and uniform multiwavelength erbium doped fiber laser using nonlinear polarization rotation," *Opt. Express*, vol. 14, pp. 8205–8510, 2006.

[30] Z. Zhang *et al.*, "Multiwavelength fiber laser with fine adjustment, based on nonlinear polarization rotation and birefringence fiber filter," *Opt. Lett.*, vol. 33, pp. 324–326, 2008.

[31] X. Feng, H.-Y. Tam, and P. K. A. Wai, "Stable and uniform multiwavelength erbium doped fiber laser using nonlinear polarization rotation," *Opt. Express*, vol. 14, pp. 8205–8510, 2006.

[32] X. M. Liu *et al.*, "Graphene-clad microfiber saturable absorber foer ultrafast fibre lasers," *Sci. Rep.*, vol. 6, 2016, Art. no. 26024.

[33] Y. K. Chen, M. C. Wu, T. Tanbun-Ek, R. A. Logan, and M. A. Chin, "Subpicosecond monolithic colliding-pulse mode-locked multiple quantum well lasers," *Appl. Phys. Lett.*, vol. 58, pp. 1253–1255, 1991.

[34] Q. kenan, Z. Weigang, L. Zhuolin, H. Shen, and L. Zhang, "Dispersion compensation in ultra-short optical pulse compressing system and transmitting system," *Chin. J. Lasers*, vol. 37, pp. 449–453, 2010.

[35] G. Sobon, J. Sotor, and K. M. Abramski, "Passive harmonic mode-locked in Er-doped fiber laser based on grapheme saturable absorber with repetition rates scalable to 2.22 GHz," *Appl. Phys. Lett.*, vol. 100, 2012, Art. no. 161109.

[36] X. Zhang, H. Hu, W. Li, and N. K. Dutta, "High-repetition-rate ultrashort pulsed fiber ring laser using hybrid mode locked," *Appl. Opt.*, vol. 55, pp. 7885–7891, 2016.

[37] J. N. Kutz, B. C. Collings, K. Bergman, and W. H. Knox, "Stabilized Pulse spacing in soliton lasers due to gain depletion and recovery," *IEEE J. Quantum Electron.*, vol. 34, no. 9, pp. 1749–1757, Sep. 1998.

[38] Y. D. Cui, F. F. Lu, and X. M. Liu, "Nonlinear saturable and polarization-induced absorption of rhenium disulfide," *Sci. Rep.*, vol. 7, 2017, Art. no. 40080.

[39] A. Haboucha *et al.*, "Mechanism of multiple pulse formation in the normal dispersion regime of passively mode-locked fiber ring lasers," *Opt. Fiber Technol.*, vol. 14, pp. 262–267, 2008.

[40] X. M. Liu, and Y. D. Cui, "Flexible pulse-controlled fiber laser," *Sci. Rep.*, vol. 5, 2015, Art. no. 09399.

[41] Y. C. Meng *et al.*, "Multiple soliton dynamic patterns in a graphene mode-locked fiber laser," *Opt. Express*, vol. 20, pp. 6685–6692, 2012.

[42] J. Peng *et al.*, "Direct generation of 128-fs Gaussian pulses from a compensation-free fiber laser using dual mode-locked mechanisms," *Opt. Commun.*, vol. 285, pp. 731–733, 2012.

[43] P. Li *et al.*, "Subpicosecond SESAM and nonlinear polarization evolution hybrid mode-locked ytterbium-doped fiber oscillator," *Appl. Phys. B*, vol. 118, pp. 561–566, 2015.

[44] A. Budnicki, L. Szpak, M. Maternia, and K. M. Abramski, "Passively mode-locked erbium doped laser with combination of NPR and NALM effects," in *Proc. Int. Conf. Transparent Opt. Netw.*, 2006, pp. 181–184.

[45] J. Qingsong *et al.*, "Mode-Locked thulium-doped fiber laser with 1.78-GHz repetition rate based on combination of nonlinear polarization rotation and semiconductor saturable absorber mirror," *IEEE Photon. J.*, vol. 9, no. 3, Jun. 2017, Art. no. 1502808.

[46] A. P. Luo, Z. C. Luo, and W. C. Xu, "Tunable and switchable multi-wavelength erbium-doped fiber ring laser based on amodified dual-pass Mach-Zehnder interferometer," *Opt. Lett.*, vol. 34, pp. 2135–2137, 2009.

[47] S. L. Pan and C. Y. Lou, "Stable multiwavelength dispersion-tuned actively mode-locked erbium-doped fiber laser using nonlinear polarization rotation," *IEEE Photon. Technol. Lett.*, vol. 18, no. 3, pp. 1451–1453, Jul. 2006.

[48] X. Feng, H. Tam, and P. K. A. Wai, "Stable and uniform multiwavelength erbium-doped fiber laser using nonlinear polarization rotation," *Opt. Express*, vol. 14, pp. 8205–8210, 2006.

[49] H. Ahmad *et al.*, "Investigation of ellipticity and pump power in a passively mode-locked fiber laser using the nonlinear polarization rotation technique," *Chin. Opt. Lett.*, vol. 15, 2017, Art. no. 051402.

[50] R. I. Woodward, and E. J. R. Kelleher, "Towards 'smart lasers': self optimization of an ultrafast pulse source using a genetic algorithm," *Sci. Rep.*, vol. 6, 2016, Art. no. 37616.

[51] R. I. Woodward, E. J. R. Kelleher, R .C. T. Howe "Tunable Q-switched fiber laser based on saturable edge-state absorption in few-layer molybdenum disulfide (MoS_2)," *Opt. Express*, vol. 22, pp. 31113–31122, 2014.

[52] Y. Meng *et al.*, "Mode-locked Er: Yb-doped double-clad fiber laser with 75-nm tuning range," *Opt. Lett.*, vol. 40, pp. 1153–1156, 2015.

[53] X. Wang *et al.*, "Tunable, multiwavelength Tm-doped fiber laser based on polarization rotation and four-wave-mixing effect," *Opt. Express*, vol. 21, pp. 25977–25984, 2013.

[54] W. Ma *et al.*, "Widely tunable 2 μm continuous-wave and mode-locked fiber laser," *Appl. Opt.*, vol. 56, pp. 3342–3346, 2017.

[55] Z. X. Zhang, Z. X. Xu and L. Zhang, "Tunable and switchable dual-wavelength dissipative soliton generation in an all-normal-dispersion Yb-doped fiber laser with birefringence fiber filter," *Opt. Express*, vol. 20, pp. 26736–26742, 2012.

[56] W. Ma *et al.*, "Wavelength-spacing switchable dual-wavelength single longitudinal mode thulium-doped fiber at 1.9 μm," *IEEE Photon. J.*, vol. 8, no. 6, Dec. 2016, Art. no. 1504508.

[57] X. Wang, P. Zhou, X. Wang, H. Xiao, and Z. Liu, "Pulse bundles and passive harmonic mode locked pulses in Tm-doped fiber laser based on nonlinear polarization rotation," *Opt. Express*, vol. 22, pp. 6147–6153, 2014.

[58] S. M. J. Kelly, "Characteristic sideband instability of periodically amplified average soliton," *IEE Electron. Lett.*, vol. 28, no. 8, pp. 806–808, Apr. 1992.

[59] M. Nakazawa, E. Yoshida, and Y. Kimura "Generation of 98 fs optical pulses directly from an erbium-doped fibre ring laser at 1-57 μm," *IEE Electron. Lett.*, vol. 29, no. 1, pp. 63–65, 1993.

[60] D. J. Richardson *et al.*, "Selfstarting, passively modelocked erbium fibre ring laser based on the amplifying Sagnac switch," *IEE Electron. Lett.*, vol. 27, no. 6, pp. 542–544, Mar. 1991.

[61] Y. Xu *et al.*, "Dissipative soliton resonance in a wavelength-tunable thulium-doped fiber laser with net-normal dispersion," *IEEE Photon. J.*, vol. 7, no. 3, pp. 1–7, Jun. 2015.

[62] S. K. Wang *et al.*, "Dissipative soliton resonance in a passively mode-locked figure-eight fiber laser," *Opt. Express*, vol. 21, pp. 2402–2407, 2013.
[63] K. Krzempek, "Dissipative soliton resonances in all-fiber Er-Yb double clad figure-8 laser," *Opt. Express*, vol. 23, pp. 30651–30656, 2015.
[64] Y. Q. Huang, Y. L. Qi, Z. C. Luo, A. P. Luo, and W. C. Xu, "Versatile patterns of multiple rectangular noise-like pulses in a fiber laser," *Opt. Express*, vol. 24, pp. 7356–7363, 2016.
[65] Y. Q. Huang *et al.*, "Coexistence of harmonic soliton molecules and rectangular noise-like pulses in a figure-eight fiber laser," *Opt. Lett.*, vol. 41, pp. 4056–4059, 2016.
[66] H. Liu *et al.*, "Generation of multiwavelength noise-like square-pulses in a fiber laser," *IEEE Photon. Technol. Lett.*, vol. 26, no. 19, pp. 1990–1993, Oct. 2014.
[67] Q. Y. Ning *et al.*, "Vector nature of multi-soliton patterns in a passively mode-locked figure-eight fiber laser," *Opt. Express*, vol. 22, pp. 11900–11911, 2014.
[68] Z. C. Luo *et al.*, "Vector dissipative soliton resonance in a fiber laser," *Opt. Express*, vol. 21, pp. 10199–10204, 2013.
[69] S. Qingchao *et al.*, "Dual square-wave pulse passively mode-locked fiber laser," *Appl. Opt.*, vol. 56, pp. 4934–4939, 2017.
[70] M. E. Fermann, F. Haberl, M. Hofer, and H. Hochreiter, "Nonlinear amplifying loop mirror," *Opt. Lett.*, vol. 15, pp.752–754, 1990.
[71] L. M. Zhao, D. Y. Tang, J. Wu, X. Q. Fu, and S. C. Wen, "Noise-like pulse in a gain-guided soliton fiber laser," *Opt. Express*, vol. 15, pp. 2145–2150, 2007.
[72] X. W. Zheng *et al.*, "High-energy noiselike rectangular pulse in a passively mode-locked figure-eight fiber laser," *Appl. Phy. Express*, vol. 7, 2014, Art. no. 042701.
[73] H. Zhang, D. Y. Tang, L. M. Zhao, and N. Xiang, "Coherent energy exchange between components of a vector soliton in fiber lasers," *Opt. Express*, vol. 16, pp. 12618–12623, 2008.
[74] Y. F. Tang, H. Zhang, D. Y. Tang, and D. Y. Shen, "Polarization rotation vector solitons in a grapheme mode-locked fiber laser," *Opt, Express*, vol. 20, pp. 27283–27289, 2012.
[75] A. B. Grudinin and S. Gray, "Passive harmonic mode locking in soliton fiber lasers," *J. Opt. Soc. Amer. B*, vol. 14, pp. 144–154, 1997.
[76] M. J Guy, D. U. Noske, and J. R. Taylor, "Generation of femtosecond soliton pulses by passive mode locking of an ytterbium-erbium figure-of-eight fiber laser," *Opt. Lett.*, vol. 18, pp. 1447–1449, 1993.
[77] F. Gutty, Ph. Grelu, N. Huot, G. Vienne, and G. Millot, "Stabilisation of modelocking in fibre ring laser through pulse bunching," *IEE Electron. Lett.*, vol. 37, no. 12, pp. 745–746, Jun. 2001.
[78] S. Chouli and P. Grelu, "Soliton rains in a fiber laser: An experimental study," *Phys. Rev. A.*, vol. 81, 2010, Art. no. 063829.
[79] S. Chouli and Ph. Grelu, "Rains of solitons in a fiber laser," *Opt. Express*, vol. 17, pp. 11776–11781, 2009.
[80] S. Wabnitz, "Control of soliton train transmission, storage, and clock recovery by CW light injection," *J. Opt. Soc. Amer. B*, vol. 13, pp. 2739–2749, 1996.
[81] J. M. Soto-Crespo, N. Akhmediev, Ph. Grelu, and F. Belhache, "Quantized separations of phase-locked soliton pairs in fiber lasers," *Opt. Lett.*, vol. 28, pp. 1757–1759, 2003.
[82] D. Y. Tang, L. M. Zhao, G. Q. Xie, and L. Qian, "Coexistence and competition between different soliton shaping mechanisms in a laser," *Phys. Rev. A*, vol. 75, 2007, Art. no. 063810.

Tianshu Wang was born in Changchun, Jilin, China, in 1975. He received the B.S. degree in electronics engineering from the Institute of Military Armored Engineering, Beijing, China, in 1998, and the M.S. and Ph.D. degree in electronics engineering from Jilin University, Changchun, China, in 2007.

From 2007 to 2009, he was a Postdoctoral Researcher with the Center for Optical and Electromagnetic Research, Zhejiang University. From 2009 to 2012, he was an Assistant Professor with the Communications Engineering College, Hangzhou Dianzi University. Since 2013, he has been a Professor with the National and Local Joint Engineering Research Center of Space Optoelectronics Technology, Changchun University of Science and Technology, Changchun, China. He has authored or coauthored more than 100 papers and a book on fiber lasers and their applications, and more than 10 inventions. His research interests include fiber laser and free space laser communications.

Wanzhuo Ma was born in Changchun, Jilin, China, in 1989. He received the B.S. and M.S. degrees in optical engineering from Changchun University of Science and Technology, Changchun, China, in 2016.

From 2016, he has been working toward the Ph.D. degree at Changchun University of Science and Technology. His research interests include ultrafast fiber laser and free-space laser communication.

Qingsong Jia was born in Yushu, Jilin, China, in 1988. He received his B.S. degree from the College of Science, Changchun University of Science and Technology, Changchun, China, in 2012, and the M.S. degree in optical engineering from the Changchun University of Science and Technology, Changchun, China, in 2015.

From 2016, he has been working toward the Ph.D. degree at Changchun University of Science and Technology. His research interests include ultrafast fiber laser and free-space laser communication.

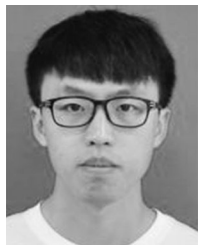

Qingchao Su was born in Baishan, Jilin, China in 1992. He received the B.S. degree from Changchun University of Science and Technology, Changchun, China, in 2015.

From 2015, he has been working toward the Master's degree at the Space Optoelectronic Technology Laboratory. His research interests include fiber lasers and space laser communication.

Peng Liu was born in Langfang, Hebei, China, in 1990. He received the B.S. and M.S. degrees in optics from Changchun University of Science and Technology, Changchun, China, in 2017.

From 2014 to 2017, he was a Master Degree Candidate with Changchun Changchun University of Science and Technology. His research focuses on fiber laser.

Peng Zhang was born in Changting, Fujian, China, in 1985. He received the B.S. degree in photonic science and technology from Changchun University of Science and Technology, Changchun, China, in 2007, and the Ph.D. degree in optical engineering from Changchun Institute of Optics and Fine Mechanics and Physics, Chinese Academy of Science, Beijing, China, in 2012.

From 2012 to 2015, he was an Assistant Professor with the National and Local Joint Engineering Research Center of Space Optoelectronics Technology, Changchun University of Science and Technology. Since 2015, he has been an Associate Professor in optical engineering with Changchun University of Science and Technology. He is the author of more than 20 articles, and an inventor of more than 5 inventions. His research interests include space optical communications and fiber laser.